

PROMPT EMISSION CALCULATIONS FOR $^{233}\text{U}(n_{\text{th}},f)$

A. TUDORA, A. MATEI

¹University of Bucharest, Faculty of Physics, P.O.Box MG-11, RO-077125 Bucharest-Magurele, Romania

E-mail: anabellatudora@hotmail.com,

E-mail: anamateiro@yahoo.ro

Received May 24, 2018

Abstract. Detailed prompt emission results of two refined models (one including the sequential emission treatment and another based on a residual temperature distribution) describing very well all experimental data of $^{233}\text{U}(n_{\text{th}},f)$ are for the first time reported. They answer to the international request of accurate nuclear fission data for the fissile nucleus of the Th-U fuel cycle.

Key words: prompt emission in fission, nuclear fission.

1. INTRODUCTION

The deep knowledge of the prompt neutron and γ -ray emission in fission is a very important request in the international context of the sustainable development concept, which re-highlights the nuclear fission as a major solution for energy needs in the near and medium future. Important applications such as those related to new reactor projects (Generation IV), the transmutation of the long-life nuclear waste, the energy sources for different devices for outer space investigations, the high power propulsion (submarines and aircraft carriers) are only a few areas which need accurate nuclear fission data. Many quantities characterizing the prompt neutron and γ -ray emission play a crucial role in applications, *e.g.* the energy release in fission (Q -value), the average number of prompt neutrons $\langle \nu \rangle$ (which enters the k_{eff} multiplication factor of nuclear reactors), the *prompt fission neutron spectrum* (PFNS) which is the weighting function of the fast neutron group etc. These quantities are basic nuclear data entering the *evaluated nuclear data libraries* (ENDF).

Accurate evaluated nuclear data for the neutron-induced fission of ^{233}U is an important requirement at international level because it is the fissile nucleus of the Th-U fuel cycle, which will be used in future applications (*e.g.* Accelerator Driven Systems).

The present work answers to this request by reporting model calculations of almost all prompt neutron and γ -ray quantities for $^{233}\text{U}(n_{\text{th}},f)$. Two deterministic prompt emission models were employed, both developed at the University of Bucharest. One is the well-known model *Point-by-Point* (PbP) (described in Ref. [1] and references therein), which has been already used for many evaluations (details can be found *e.g.* in Ref. [2] and references therein). The PbP model is based on a global treatment of the sequential emission by considering a residual temperature distribution with a triangular form. The other model, recently developed, see Ref. [3],

includes a detailed sequential emission treatment based on recursive equations of residual temperatures. The results for $^{233}\text{U}(\text{n}_{\text{th}},\text{f})$ of both models are validated by the very good description of multi-parametric experimental data of prompt neutron multiplicity $\nu(A, \text{TKE})$ and other experimental single distributions of prompt neutrons and γ -rays ($\nu(A)$, $\nu(\text{TKE})$, $E\gamma(A)$, $N\gamma(A)$).

In the last years many efforts were addressed to the experimental investigation of prompt γ -ray emission of major actinides (see *e.g.* Refs. [4, 5] and references therein). The most recent measurements performed in February 2018 at the Budapest research reactor VVR by a team including scientists from ELI-NP Romania, EC JRC-Geel Belgium, IPN Orsay France, has concerned the fissioning system $^{233}\text{U}(\text{n}_{\text{th}},\text{f})$. The processing of measured data of this experiment is in progress. The model results of prompt γ -ray emission obtained in this work can be useful in the processing data mentioned above.

2. BRIEF REVIEW OF PROMPT EMISSION MODELS USED IN THIS WORK

Both the PbP and the sequential emission modelings take into account a large range of fragmentations and *total kinetic energy* (TKE) deterministically constructed as follows. A large fragment mass range going from symmetric fission up to a very asymmetric split, with a step of 1 mass unit is taken into account. For each fragment mass number A three charge numbers Z are considered as the nearest integer values above and below the most probable charge Z_p taken as unchanged charge distribution (UCD) corrected with the charge polarization, *i.e.* $Z_p(A) = Z_{\text{UCD}}(A) + \Delta Z(A)$. In the case of $^{233}\text{U}(\text{n}_{\text{th}},\text{f})$ the charge polarization $\Delta Z(A)$ and the root-mean-square $\text{rms}(A)$ of the isobaric charge distribution (taken as a narrow Gaussian function centered on $Z_p(A)$) provided by the Z_p model [6] were used. For each fragmentation a large range of *total kinetic energy* (TKE) is considered (*e.g.* going from 100 to 200 MeV with a step size of 5 MeV).

In both treatments the partition of *total excitation energy* (TXE) between fully accelerated fragments is based on the same modeling at scission. This includes the calculation of fragment extra-deformation energy at scission and the partition of the available excitation energy based on statistical equilibrium at scission and level densities of nascent fragments in the Fermi-gas regime. More details about this modeling at scission are given in Refs. [7–9].

In the PbP model the sequential emission is globally taken into account by a residual temperature distribution $P(T)$ with a triangular shape, which depends only on the nuclear temperature of initial fragments. The center-of-mass energy spectrum of prompt neutrons $\Phi(\epsilon)$ is then obtained by integrating the center-of-mass energy spectrum for a given residual temperature $\Phi(\epsilon, T)$ over the distribution $P(T)$. A comprehensive description of the PbP model is given in Ref. [1].

The same prescriptions concerning the compound nucleus cross-section of the inverse process of neutron evaporation from fragments $\sigma_c(\epsilon)$ and the level density parameters of fragments as in the majority of PbP model calculations, are

used in the present case, too. *I.e.* $\sigma_c(\varepsilon)$ provided by optical model calculations with the potential parameterization of Becchetti-Greenlees [10] and energy-dependent level density parameters provided by the super-fluid model with shell corrections of Möller and Nix [11] and the parameterization of Ignatiuk [12] for the dumping of shell effects and asymptotic level density parameter.

The primary results of the PbP model are the so-called multi-parametric matrices of different quantities, generically labeled $q(A,Z,TKE)$, characterizing both, the fission fragments and the emission of prompt neutrons and γ -rays. The comparison of such multi-parametric results with experimental data (when they exist) constitutes the most relevant validation of the model itself because the fission fragment distributions are not involved.

The previous sequential emission modelings included in the computer codes FIFRELIN, CGMF and FREYA (described in the comprehensive paper [2]) and the semi-empirical code GEF [13] are exclusively based on a probabilistic Monte-Carlo treatment. The new modeling described in Ref. [3] includes a deterministic treatment of the sequential emission which is based on recursive equations of residual temperatures. Different quantities characterizing the residual nucleus and the prompt emission (generically labeled $q_k(A,Z,TKE)$) are obtained for each emission sequence indexed k , where k is running over the number of prompt neutrons emitted successively (or the number of residual fragments) corresponding to each initial fragment $\{A, Z\}$ at each TKE value covering the fragmentation and TKE ranges (constructed as mentioned above). The multi-parametric matrices $q(A,Z,TKE)$ corresponding to an initial fragment A, Z at a TKE value are then obtained by averaging the respective quantities corresponding to an emission sequence $q_k(A,Z,TKE)$ over the number of sequences (*i.e.* the number of neutrons emitted successively from an initial fragment A, Z at a TKE value).

The recursive equations of residual temperatures can be solved under the approximations of non-energy dependent level density parameters and an analytical expression of $\sigma_c(\varepsilon)$. As it was demonstrated in Ref. [3] the $\sigma_c(\varepsilon)$ expression based on the s-wave neutron strength function parameterization depending on the mass number leads to average prompt neutron energies in the center of mass frame $\langle\varepsilon\rangle(T)$ which deviate less than 4% from the ones obtained with $\sigma_c(\varepsilon)$ from optical model calculations. The level density parameters provided by the Egidy-Bucurescu systematic for the back-shift Fermi-gas (BSFG) model can approximate well the energy-dependent level density parameters of the super-fluid model for a great part of initial and residual fragments. More details about this sequential emission modeling and its successful application to many fissioning nuclei (*i.e.* $^{252}\text{Cf}(\text{SF})$, $^{236-244}\text{Pu}(\text{SF})$, $^{235}\text{U}(\text{n}_{\text{th}},\text{f})$, $^{239}\text{Pu}(\text{n}_{\text{th}},\text{f})$, $^{237}\text{Np}(\text{n},\text{f})$, $^{238,234}\text{U}(\text{n},\text{f})$ up to an incident neutron energy of about 5 MeV) are given in Ref. [3].

Different quantities (characterizing the fragments and the prompt emission) as a function of initial fragment mass A , $q(A)$, as a function of TKE , $q(TKE)$, and total average quantities $\langle q \rangle$ are obtained by averaging the corresponding multi-parametric matrices $q(A,Z,TKE)$ provided by both modelings, over the $Y(A,Z,TKE)$ distribution of fission fragments (by summing over Z and TKE and over A and Z ,

respectively, and over A , Z and TKE in the case of total average quantities). The comparison of such quantities with existing experimental data (e.g. $\nu(A)$, $\nu(TKE)$, $\langle \varepsilon \rangle(A)$, $E\gamma(A)$, $\langle \nu \rangle$, $\langle E\gamma \rangle$ etc.) can be also considered as a valuable validation of the prompt emission model together with the fragment distribution. The multiple fission fragment distributions are based on experimental $Y(A, TKE)$ data, being taken as $Y(A, Z, TKE) = p(Z, A) Y_{exp}(A, TKE)$ (where $p(Z, A)$ is the Gaussian isobaric charge distribution mentioned above). When the experimental matrix $Y_{exp}(A, TKE)$ is not available, it can be re-constructed from available experimental data of the single distributions $Y(A)$, $TKE(A)$ and $\sigma_{TKE}(A)$. (for details see Ref. [2] and references therein). This is the case of $^{233}\text{U}(n_{th}, f)$ for which only experimental data of single distributions are available in the EXFOR library [14].

3. RESULTS AND DISCUSSIONS

Fortunately in the case of $^{233}\text{U}(n_{th}, f)$ experimental data of the double distribution of prompt neutron multiplicity $\nu(A, TKE)$ exist (measured by Nishio [15]). These data allow a proper validation of the prompt emission models themselves (the experimental $Y(A, TKE)$ distributions being not involved).

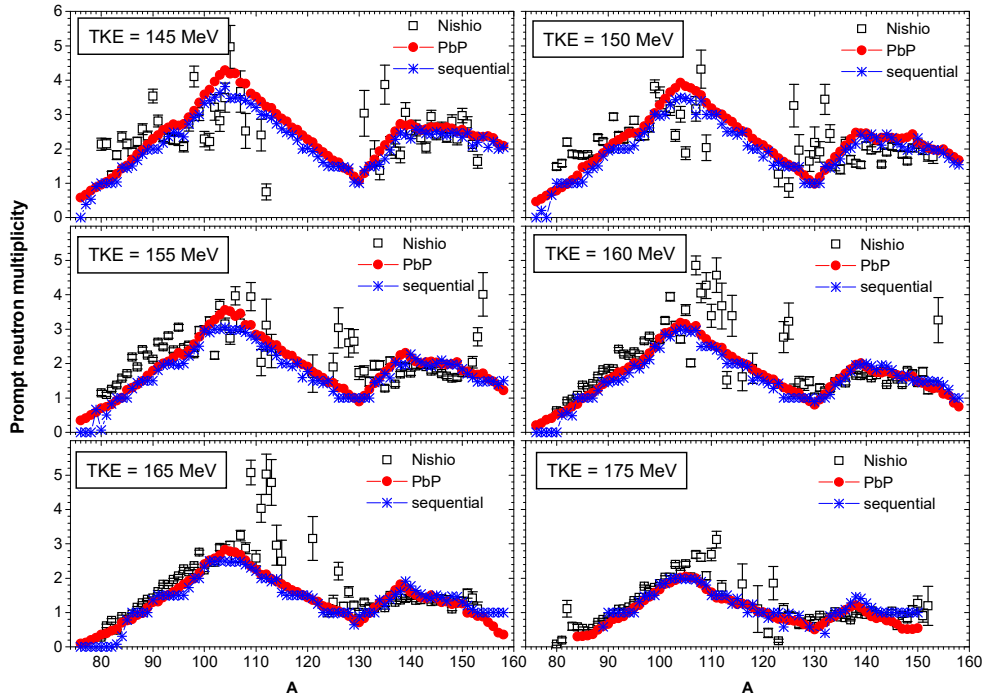


Fig. 1 – Examples of $\nu(A, TKE)$ results provided by the PbP model (full red circles) and the sequential emission treatment (blue stars) in comparison with the experimental data of Nishio (open squares), plotted as $\nu(A)$ at a given TKE value indicated in each frame (Color online).

The $\nu(A, TKE)$ results of both modelings gives a very good description of the experimental data of Nishio [15] as it can be seen in the following figures in which the matrices are given in two representations, *i.e.* as $\nu(A)$ at a given TKE value (Fig.1) and as $\nu(TKE)$ for a given fragmentation (Fig. 2). Figure 1 exemplifies $\nu(A)$ for six TKE values (indicated in each frame): the experimental data with open black squares, the PbP result with full red circles and the sequential emission result with blue stars. The saw-tooth shape of $\nu(A)$ is visible at all TKE values. The PbP and sequential emission results are close to each other and describe very well the experimental data over the entire A range, except the spread data at A near the symmetric fragmentation.

The prompt neutron multiplicities as a function of TKE for nine fragmentations (randomly chosen) are given in Fig. 2.

They are compared with the experimental data separately, *i.e.* the PbP results in the upper part and the sequential emission results in the lower part. The mass numbers A_H , A_L or each fragmentation are given in each frame. The model results are plotted with continuous lines colored in green (light fragments), blue (heavy fragments) and red (fragment pairs) and the experimental data with open black squares (light fragments), full gray circles (heavy fragments) and full black diamonds (fragment pairs). Both model results give a good description of experimental data at TKE above 140 MeV. At lower TKE values the data are very spread and exhibit a decreasing behaviour, which is the effect of the processing data, as demonstrated by Gök *et al.* [16]). The $\nu(A, TKE)$ results of sequential emission exhibit a slight staggering which succeeds to reproduce very well the staggering of experimental data, especially the data corresponding to fragment pairs (black diamonds). The staggering disappears in the case of PbP results, which exhibit a smooth behaviour due to the global treatment of the sequential emission by the use of a residual temperature distribution. In the case of spontaneous fission and neutron-induced fission at low energies it is well known that for fragmentations with mass numbers going from symmetric fission up to about the most probable fragmentation (*i.e.* A_H around 140) the light fragments emit more neutrons than the complementary heavy ones. Almost equal numbers of neutrons are emitted by the complementary fragments of the most probable fragmentation. The situation is reversed for fragmentations with A_H above 140 when the heavy fragments emit more neutrons than the complementary ones. This behaviour is confirmed by the results of Fig. 2 where $\nu_L(A, TKE)$ (green lines) is higher than $\nu_H(A, TKE)$ (blue lines) for the pairs with A_H up to about 138, the blue and green lines almost cover each other for fragmentations with A_H near 140, and the situation is reversed, *i.e.* $\nu_H(A, TKE)$ higher than $\nu_L(A, TKE)$, for fragment pairs with A_H above 140.

In Fig. 3 the prompt neutron single distributions $\nu(A)$ (upper part) and $\nu(TKE)$ (lower part) obtained by averaging the $\nu(A, TKE)$ results of both modelings over the experimental $Y(A, TKE)$ distribution of fission fragments [14] are given with full red circles (PbP) and blue stars (sequential emission) in comparison with the experimental data (different black and gray open symbols or symbols with a cross inside).

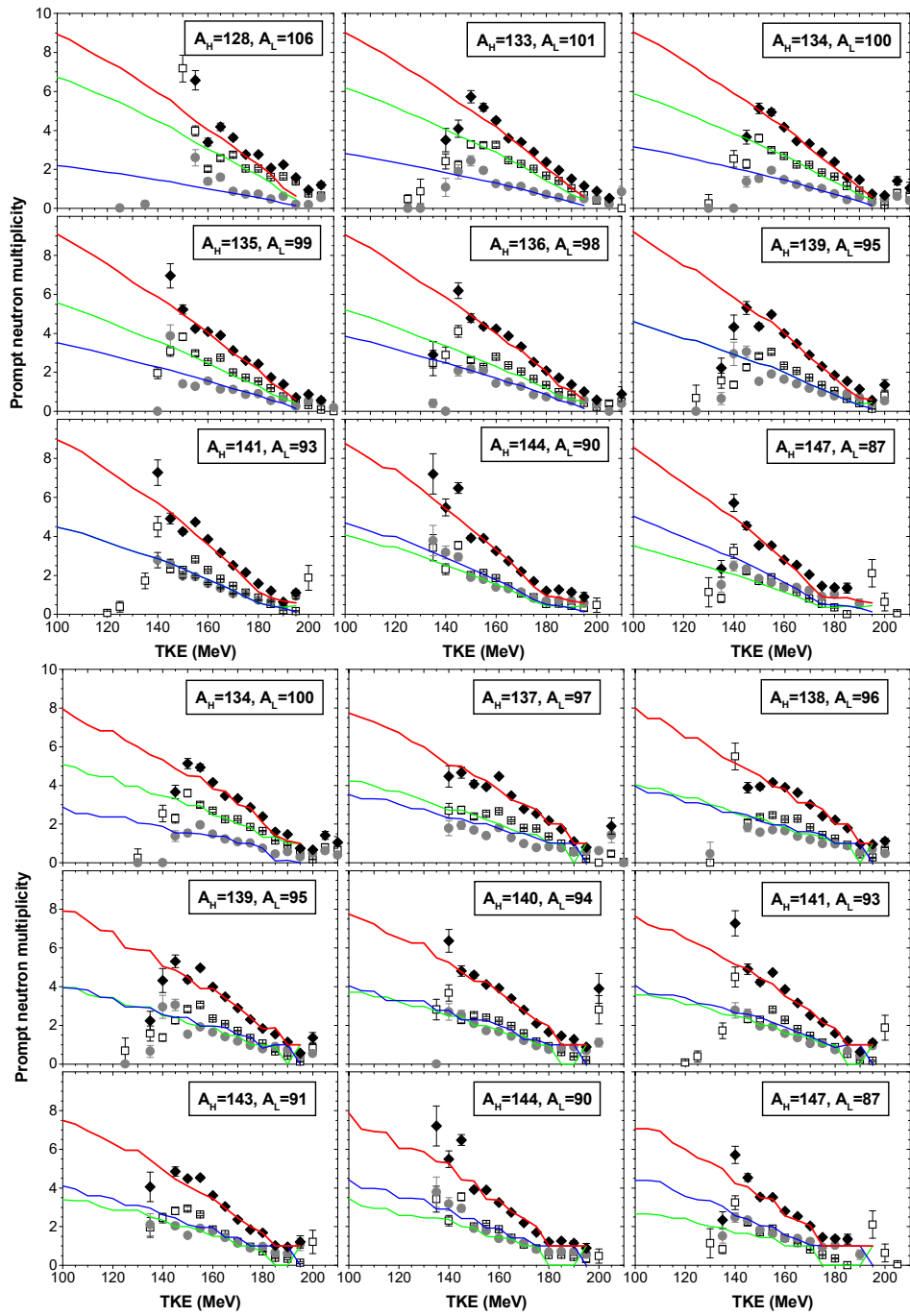


Fig. 2 – $\nu(A, TKE)$ results of PbP (upper part) and sequential emission (lower part) plotted with continuous lines in comparison with the experimental data of Nishio (symbols).

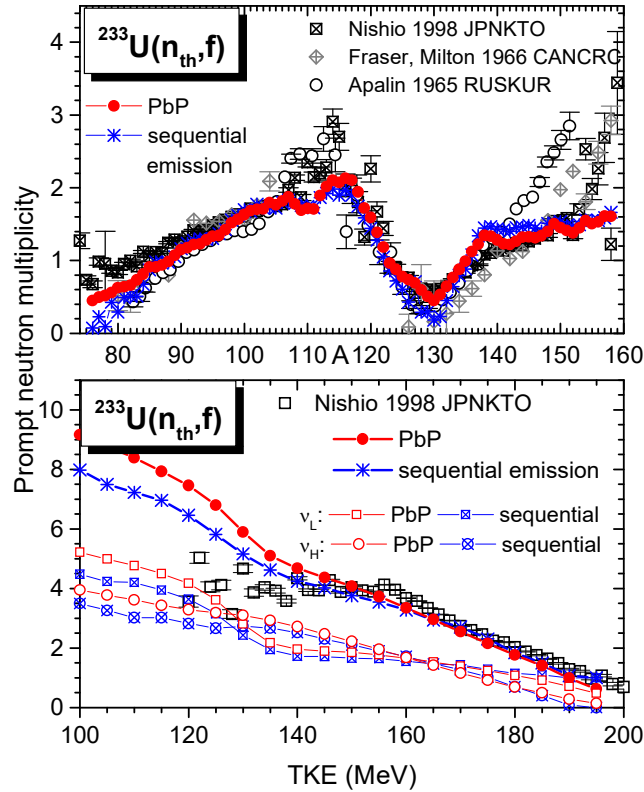


Fig. 3 – PbP (full red circles) and sequential emission (blue stars) results of $\nu(A)$ (upper part) and $\nu(TKE)$ (lower part) in comparison with the experimental data (different black and gray open symbols and symbols with a cross inside) (Color online).

As it can be seen in the upper part, the $\nu(A)$ results of PbP and sequential emission treatment are close to each other and describe well the experimental data over the entire mass range except the region of very asymmetric fragmentations, *i.e.* at A less than 90 they describe the data of Fraser and Milton and of Apalin and at A above 150 they underestimate the unphysical increase of all data. The minimum of $\nu(A)$ at A_H around 130 (due to the magic and double magic heavy fragments with $N = 82$ and $Z = 50$) is more pronounced in the case of sequential emission treatment (being in agreement with the data of Fraser and Milton) compared to the PbP result (which is in agreement with the data of Nishio and Apalin).

The $\nu(TKE)$ results of both modelings (lower part) are close to each other and in reasonable agreement with the data of Nishio for TKE above 140 MeV. They exhibit the same decreasing slope as the experimental data. Obviously, at low TKE values (below 140 MeV) the behaviour of these experimental data (due to the processing of data, as explained by Göök *et al.* [16]) is not described by the model results, which exhibit a normal trend of an almost linear decrease with increasing

TKE . The $\nu(TKE)$ result of sequential emission is lower than the PbP result at low TKE values because of the limited number of initial fragments taken at each A for which the successive neutron emission is considered, while in the case of PbP this is not happening, the global treatment by the residual temperature distribution assuring a complete sequential emission.

The experimental prompt γ -ray data especially regarding the distributions of different prompt γ -ray quantities (e.g. average prompt γ -ray energy E_γ and multiplicity N_γ) as a function of A or TKE are very scarce, being measured only for a few fissioning nuclei, the fissioning system $^{233}\text{U}(n_{th},f)$ being one of these.

The $E_\gamma(A)$ and $N_\gamma(A)$ results of the PbP model (full red circles) and of the sequential emission treatment (blue stars) describe very well the experimental data of Pleasonton [17] (black open squares) as it can be seen in the upper and lower part of Fig. 4. Again it can be seen that the deterministic treatment of the sequential emission leads to a staggering of both $E_\gamma(A)$ and $N_\gamma(A)$ while in the case of the PbP model, the global treatment of the sequential emission by the use of a triangular residual temperature distribution assures a smooth behaviour of these prompt γ -ray quantities.

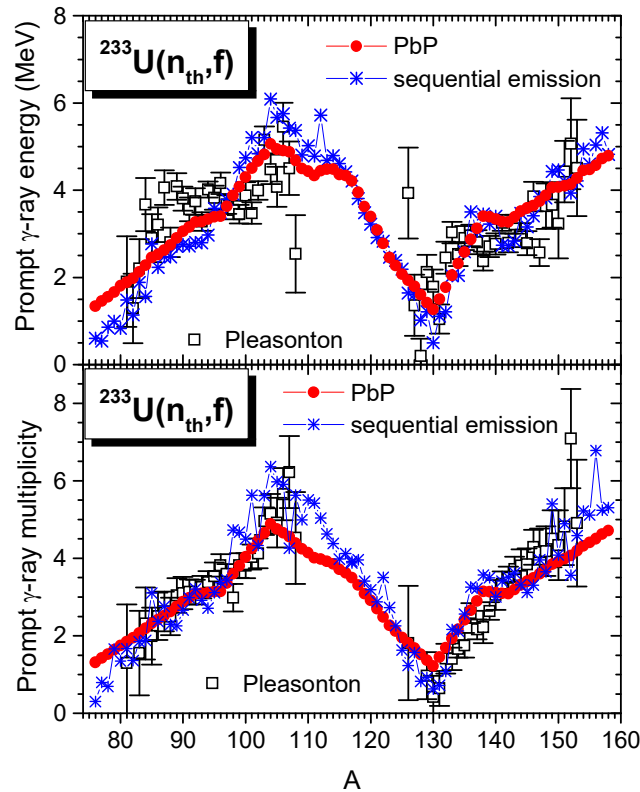


Fig. 4 – PbP (full red circles) and sequential emission (blue stars) results of $E_\gamma(A)$ (upper part) and $N_\gamma(A)$ (lower part) in comparison with the experimental data of Pleasonton (open squares) (Color online).

A linear correlation between the prompt γ -ray energy and the prompt neutron multiplicity exists. This correlation was firstly experimentally observed by Nifenecker *et al.* for the case of $^{252}\text{Cf}(\text{SF})$ [18] and Fréhaut for the neutron induced fission of ^{232}Th , ^{235}U and ^{237}Np [19]. They have reported slope and intercept values of this linear correlation for each of the investigated fissioning nuclei. A systematic for the slope and the intercept of this linear correlation (expressed only as a function of the charge and mass numbers of the fissioning nucleus) was developed by Vladuca and Tudora [20, 21].

The linear correlation resulting from the present results of $\nu(\text{TKE})$ and $E_{\gamma}(\text{TKE})$ is plotted with full red circles in Fig. 5. Its linear fit is given with a continuous red line. The linear dependence provided by the systematic of Vladuca and Tudora is plotted with a black dashed line. The very good agreement of the linear correlation resulting from the present calculation with the one of the systematic is visible.

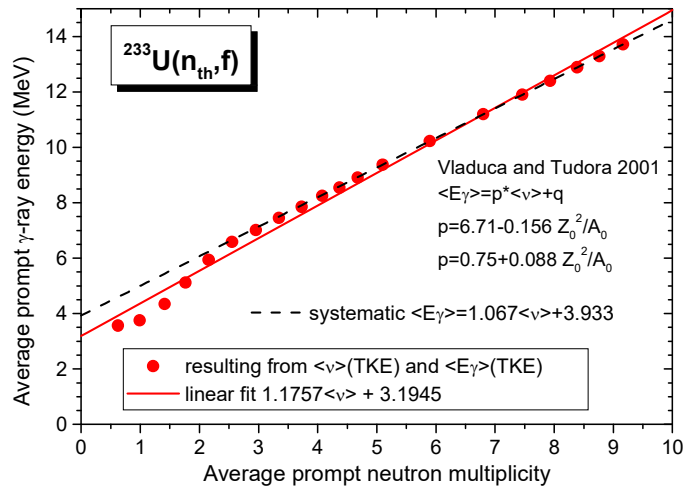


Fig. 5 – The linear correlation between E_{γ} and ν resulting from the present $E_{\gamma}(\text{TKE})$ and $\nu(\text{TKE})$ calculations (full red circles) and its linear fit (solid red line) in comparison with the systematic of Valduca and Tudora (dashed black line) (Color online).

The total average prompt neutron multiplicity $\langle \nu \rangle$ is obtained by averaging the matrices $\nu(A, \text{TKE})$ provided by the PbP and sequential emission modelings (exemplified in Figs. 1 and 2) over the experimental fragment distributions [14]. The resulting values $\langle \nu \rangle_{\text{PbP}} = 2.481$ and $\langle \nu \rangle_{\text{seq.em.}} = 2.516$ are in very good agreement with the experimental data from EXFOR and the values given in the last released versions of evaluated nuclear data libraries [22] (of 2.479 in ENDF/B-VIII, 2.489 in JEFF3.3 and 2.478 in JENDL4).

The values of total average prompt γ -ray energy and multiplicity (obtained by averaging the model results of the multi-parametric matrices of E_{γ} and N_{γ} over

the fragment distributions [14]) are in very good agreement with the experimental data as it can be seen in Table 1.

Table 1

The Present results of $\langle E\gamma \rangle$ and $\langle N\gamma \rangle$ in comparison with the experimental data

Quantity	Experim. data [17]	PbP	Sequential em.
$\langle E\gamma \rangle$ (MeV)	6.69 ± 0.3	6.581	6.480
$\langle N\gamma \rangle$	6.31 ± 0.3	6.197	6.577

Taking into account the good description of all experimental data by the prompt emission results of both modelings, a reliable prediction of these models for other prompt emission quantities of $^{233}\text{U}(n_{\text{th}},f)$ (for which the experimental information is missing).

4. CONCLUSIONS

Model calculation results of many quantities characterizing the prompt neutron and γ -ray emission of $^{233}\text{U}(n_{\text{th}},f)$ are for the first time reported.

Two deterministic treatments of prompt emission developed at the University of Bucharest, *i.e.* the Point-by-Point model (with a global treatment of the sequential emission by using a residual temperature distribution) and a new modeling including a detailed treatment of the successive emission of prompt neutrons and γ -rays (based on recursive equations of the residual temperatures) are used.

The very good description of the experimental double distribution of prompt neutron multiplicity $\nu(A, \text{TKE})$ by both model results constitutes the most relevant validation of the modelings themselves.

Other single distributions of prompt neutron multiplicity, $\nu(A)$ and $\nu(\text{TKE})$, of prompt γ -ray energy $E\gamma(A)$ and multiplicity $N\gamma(A)$ provided by both modelings are also in very good agreement with the experimental data, this being a supplementary reliable validation of the models together with the fragment distributions $Y(A, \text{TKE})$ used. The obtained values of total average prompt neutron multiplicity and of total prompt γ -ray energy and multiplicity are also in very good agreement with the experimental data and the data from the last released evaluated nuclear data libraries.

The prompt γ -ray results reported in this work can be useful in the processing of measured data of a recent experiment devoted to the prompt γ -ray emission of $^{233}\text{U}(n_{\text{th}},f)$, performed at the Budapest research reactor by an international team (including experimentalists from ELI-NP and a master student from the University of Bucharest).

Acknowledgements. This work was done in the frame of the Romanian research project PN-III-P4-PCE-2016-0014, contract 7/2017.

REFERENCES

1. A. Tudora and F.-J. Hamsch, *Eur. Phys. J. A*, **53**(8), 159 (2017).
2. R. Capote, Chen Y.J., F.-J. Hamsch, N.V. Kornilov, J.P. Lestone, O. Litaize, B. Morillon, D. Neudecker, S. Oberstedt, T. Ohsawa, N. Otuka, V.G. Pronyaev, A. Saxena, O. Serot, O.A. Shcherbakov, N.C. Shu, D.L. Smith, P. Talou, A. Trkov, A.C. Tudora, R. Vogt, S. Vorobyev, *Nucl. Data Sheets* **131**, 1–106 (2016).
3. A. Tudora, F.-J. Hamsch, V. Tobosaru, *Revisiting the residual temperature distribution in prompt neutron emission in fission*, *Eur. Phys. J. A* (2018) in press.
4. A. Oberstedt, R. Billnert, A. Gatera, A. Göök, S. Oberstedt, *EPJ Web of Conferences* **169**, 00014 (2018).
5. A. Gatera, A. Göök, F.-J. Hamsch, A. Moens, A. Oberstedt, S. Oberstedt, G. Sibbens, D. Vanleeuw, M. Vidali, *EPJ Web of Conferences* **169**, 00003 (2018).
6. A. C. Wahl, *At. Data Nucl. Data Tables* **39**, 1–156 (1988).
7. C. Morariu, A. Tudora, F.-H. Hamsch, S. Oberstedt, C. Manaiescu, *J. Phys. G: Nucl. Part. Phys.* **39**, 055103 (2012).
8. A. Tudora, F.-J. Hamsch, I. Visan, G. Giubega, *Nucl. Phys. A* **940**, 242–263 (2015).
9. I. Visan, G. Giubega, A. Tudora, *Rom. Rep. Phys.* **67**, 483–493 (2015).
10. RIPL-3 Reference Input Parameter Library of IAEA, segment IV *Optical model parameters*, Becchetti-Greenlees. Available online at <https://www-nds.iaea.org>.
11. RIPL-3 Reference Input Parameter Library of IAEA, segment I *Nuclear masses and deformations*, database of Möller and Nix. Available online at <https://www-nds.iaea.org>.
12. A. V. Ignatiuk in IAEA-RIPL1-TECDOC-1034, Segment V, chapt.5.1.4 (1988).
13. K.-H. Schmidt, B. Jurado, C. Amouroux, C. Schmitt, *Nucl. Data Sheets* **131**, 107–221 (2016).
14. EXFOR Experimental Nuclear Data Library (available online <https://www-nds.iaea.org>), target U-233, reaction (n, f), entries 40112004 (Y(A)), 40112007 (TKE(A)), 21771014 (TKE(A), $\sigma_{\text{TKE}}(A)$).
15. EXFOR Experimental Nuclear Data Library (available online <https://www-nds.iaea.org>), target U-233, reaction (n, f), quantity MFQ, data of Nishio (entries 2266005, 2266007, 2266008), Apalin (entry 41397004), Fraser and Milton (entry 14369004).
16. A. Göök, F.-J. Hamsch, M. Vidali, *Phys. Rev. C* **90**, 064611 (2014).
17. F. Pleasonton, *Nucl. Phys. A* **213**, 413–425 (1973).
18. H. Nifenecker, C. Signarbieux, R. Babinet, J. Poitou, *Neutron and gamma emission in fission*, IAEA-SM-174/207 review paper (1973).
19. J. Fréhaut, IAEA-INDC(NDS)-220, 99–111 (1989).
20. G. Vladuca and A. Tudora, *Ann. Nucl. Energy* **28**, 419–435 (2001).
21. A. Tudora, *Ann. Nucl. Energy* **36**, 72–84 (2009).
22. Evaluated Nuclear Data Libraries ENDF/B-VIII, JEFF3.3, JENDL4 (available online <https://www-nds.iaea.org>), ZA92233, file MF=1. MT=456.